The SQUID Controller Unit for the LiteBIRD Space Mission: Description, Functional Tests and Early Performance Assessment

Giulia Conenna[1,2] · Andrea Tartari[3] · Giovanni Signorelli[3,4] · Andrea Passerini[1,2] ·
Andrea Limonta[1,2] · Mario Zannoni[1,2] · Paolo Dal Bo[3,4] · Eugenia Di Giorgi[3,4] ·
Jean-François Cliche[5] · Stefano Della Torre[2] · Matt Dobbs[5] · Luca Galli[3] ·
Massimo Gervasi[1,2] · Maurizio Massa[3] · Andrea Moggi[3] · Joshua Montgomery[5] ·
Donato Nicolò[3] · Michele Pinchera[3] · Graeme Smecher[6] · Franco Spinella[3]

Abstract

LiteBIRD is a satellite mission to be launched by JAXA in the early 2030s. It will measure the Cosmic Microwave Background (CMB) primordial B-modes with an unprecedented sensitivity. Microwave radiation will be detected by Transition Edge Sensors (TESs) arrays multiplexed in frequency domain and read by Superconducting QUantum Interference Devices (SQUIDs). The LiteBIRD SQUID Controller Unit (SCU), based on the heritage of the successful design used for the ground-based SPT3G experiment, presents some novel elements that make it suitable for a space-borne application. We compare our first breadboard model with the ground-based, Off-The-Shelf Components (COTS) version, by driving the same SQUID Array Amplifier (SAA) at 4 K, measuring relevant quantities such as noise, gain and bandwidth. We demonstrate that the noise added by our first prototype (including a switching part for redundancy purposes) never exceeds the noise added by the COTS-based electronics board, representing our benchmark. We also present the first noise estimates with the SAA cooled below 1 K, going closer to the conditions expected for LiteBIRD operation.

1 Introduction

LiteBIRD, the lite (Light) satellite for the study of B-mode polarization and Inflation from cosmic background Radiation Detection, is the next-generation satellite for the observation of the Cosmic Microwave Background (CMB). It will be launched in the early 2030s by a JAXA H3 rocket [1] and inserted into an orbit around the Sun-Earth

---

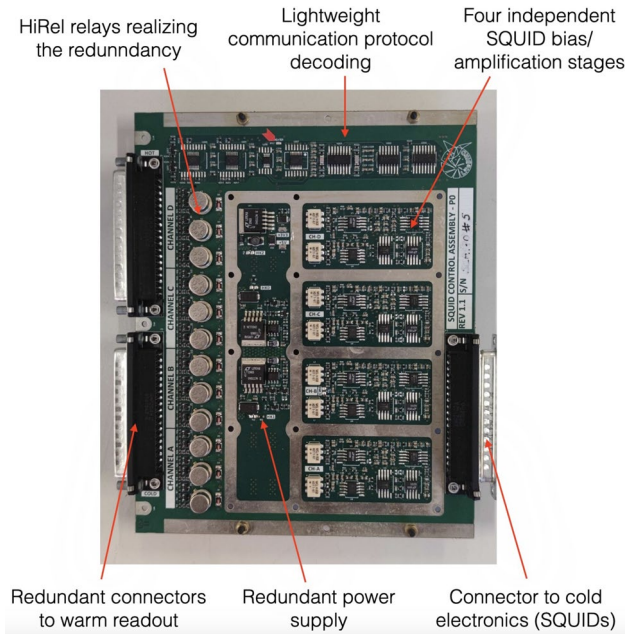Extended author information available on the last page of the article

Fig. 1 Picture of one of the version of the SCA: SCA#5 prototype, with relays in all the channels

Lagrangian point L2. It is planned to carry out three years of observations. Up to now, the most recent constraint on the tensor-to-scalar ratio, r, which is proportional to the B-mode power, is $r < 0.032$ [2, 3] and the LiteBIRD mission requirement is to measure r with a total uncertainty of $\delta r < 10^{-3}$. The LiteBIRD payload module hosts three telescopes [4], the low frequency telescope, LFT (34–161 GHz), the middle frequency telescope, MFT (89–225 GHz), and the high frequency telescope, HFT (166–448 GHz). The three telescopes' focal planes, cooled down to 0.1 K, are populated by multi-chroic polarization-sensitive antennas read by TESs, totalling 4508 detectors. TESs are coupled to arrays of superconducting LC filters to be multiplexed in the frequency domain, each array (68x) is read by one Superconducting QUantum Interference Device (SQUID) [5]. This constitutes the so-called cold readout electronics. The warm readout electronics is composed of the SQUID Controller Unit (SCU), made of up to eight SQUID Controller Assemblies (SCAs) (an example in Fig. 1), each of it driving and reading four SQUID array amplifiers, and by the Signal Processing Units (SPUs) that perform the signal processing required to operate the TESs.

2 The SQUID Controller Unit (SCU)

The SQUID Controller Unit (SCU) to control LiteBIRD SQUIDs is based on the heritage of the successful design used for the ground-based SPT-3G experiment [6]. The latter uses Commercial Off-The-Shelf (COTS) components; however, its design is further developed with some novel elements that make it suitable for a
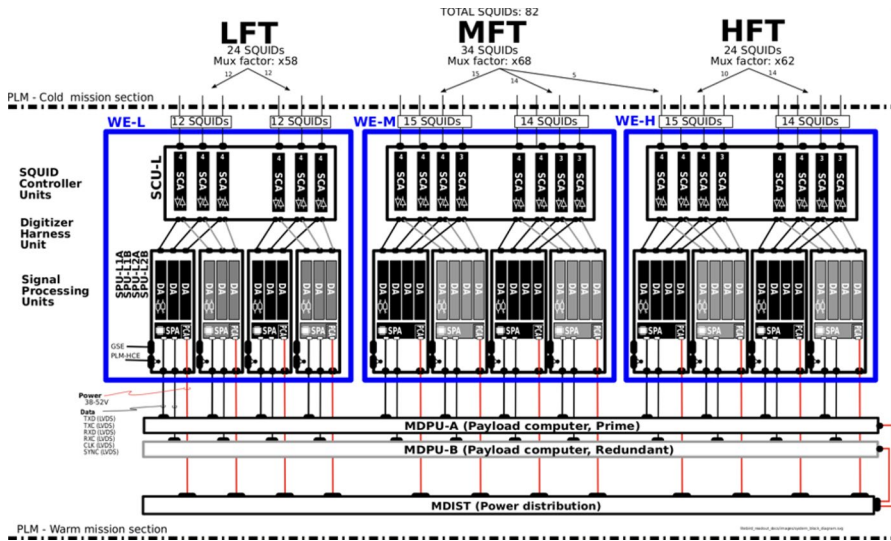
Fig. 2 Warm readout electronics architecture. The digital process units are redundant so each SCA has a double I/O

space-borne application. In particular, we have implemented support for redundancy in the Signal Processing Units (SPU), based on components available in space-grade version, and we have developed a light-weight communication protocol that is both fast and reliable. Redundancy is both given by the presence of two identical power supplies and by doubling the signal path towards two digital boards, acting as hot and cold spares. These signals are routed to the operative board by means of a set of Teledyne bi-stable relays (model 422K-5). In this way, each SCU can talk to the two different SPUs (upstream from the SCUs in the electronics architecture of Lite-BIRD) and switch from the main spare to the redundant one in case of failure (see Fig. 2).

3 SQUID Controller Assembly Tests

In a single SCU, there are up to eight SQUID Controller Assemblies (SCAs). Each SCA can control four SQUID array amplifiers: channels A, B, C, D. When relays are mounted, the nominal/main channel is called, in what follows, the hot one, while the spare is the cold one.

3.1 Warm Test–Preliminary Tests

Three kinds of tests are envisaged for each SCA: electrical, functional (*e.g.* DAC range, communication, bandwidth) and performance (readout noise) tests. Bench-top tests of the SCA are performed using an ancillary test board based on an Xilinx
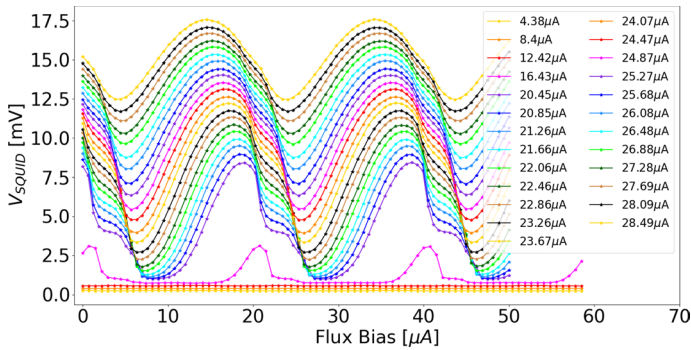
Fig. 3 V-Φ curves at different current biases

Artix-7 FPGA (Digilent Cmod A7), mimicking the signal processing boards. After successful electrical and warm functional tests performed at INFN Milano Bicocca and INFN Pisa, we carried out performance tests at McGill University, Montreal, where a dilution cryostat hosts a representative cold electronics chain. Thorough noise investigation is important to understand the system performance [7]. We present here a preliminary characterization and a simplified model of our system.

3.2 Performance Test Configurations

Two SCA boards were tested (named SCA#3 and SCA#4) plugged to a cold readout section in the McGill cryogenic test facility. SCA#3 has relays installed on channels A &B while SCA#4 has relays installed on channels C &D. In this way, we could compare noise figures both between nominal and redundant channels, and between channels with/without relay, as well as comparing the noise performance of our boards with the COTS board.

In particular, channel-B was connected to a NIST SA20 SQUID Series Array[1] (SSA) coupled to a representative 68x multiplexing chip with resistors in the 1Ω to 4Ω range (mimicking the TESs) cooled down to about 1 K.

In Fig. 3, we report typical characteristics of the SA20 SQUID read by the SCA. From V-Φ values, we extract both transimpedance (Z_{trans}) and the dynamical resistance (R_{dyn}) for significant bias current values (i.e. between $\sim 21\ \mu A$ and $\sim 26\ \mu A$), at a fixed flux bias ($\sim 31.6\ \mu A$, see Fig. 9 later in the paper). We use only the positive slope of the V-Φ since the negative one shows a distorted behaviour, visible only at low SQUID temperature, which is now understood (see e.g. [8]) and whose mitigation is in progress.

---

[1] The SQUID to be used in LiteBIRD has not been selected yet. NIST SA20 has some properties, such as high amplification and low dissipation power, that makes it one of the possible candidates, although a dedicated R &D activity is ongoing for the SQUID selection.
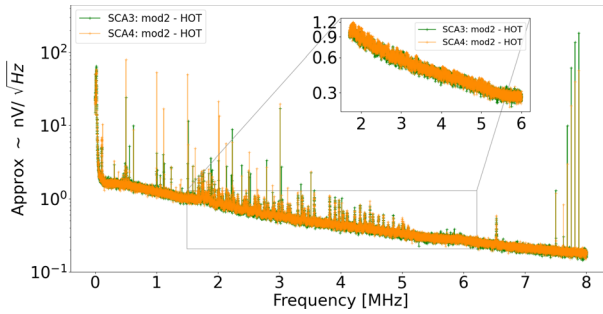
Fig. 4 Noise figure, configuration comparison: relay (SCA#3, green) vs non-relay (SCA#4, orange). The total level of noise with the tones is in the main box, while in the smaller one we plot the baselines noise (removing peaks) in a frequency range between ~2 and ~6 MHz
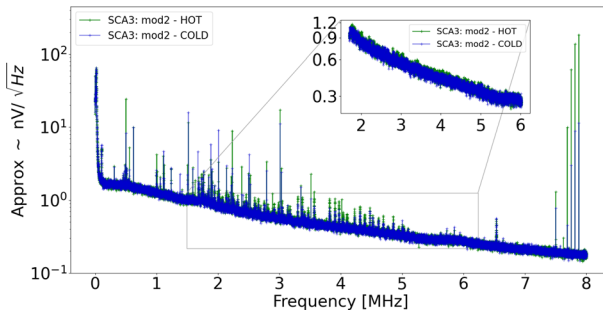

Fig. 5 Noise figure, configuration comparison: main relay (SCA#3-HOT, green) versus redundant relay (SCA#3-COLD, blue). The total level of noise with the tones is in the main box, while in the smaller one we plot the baselines noise (removing peaks) in a frequency range between ~2 and ~6 MHz

The SQUID was then biased at a convenient point (~23 μA, with flux bias ~31.6 μA) and the noise at SQUID output (in nV/$\sqrt{\text{Hz}}$) was evaluated by reading its output value as a function of the frequency in absence of any input signal.

We evaluated the total level of the SQUID output noise to compare the performance of the SCA boards in different settings. In particular, we considered the range 1.5 MHz to 5.5 MHz, where the tones of the frequency-domain multiplexing are placed. In that range, we extracted the noise baselines for a straightforward comparison by filtering out the tones. The compatibility between two different configurations is evaluated by subtracting the averaged baselines squared and by comparing the results with zero. We compare: switched (relay) versus hard-wired channels (no relay) in Fig. 4; main (hot) vs redundant (cold) board channel in Fig. 5; INFN board (4 units, including redundancy) vs COTS board used in the ground-based SPT-3G experiment, in Fig. 6. As explained in the following Sect. 4, the absolute noise value (affected by the attenuation of the overall chain) is still under evaluation, and for this reason, the noise figures are labelled as "Approx ~ nV/$\sqrt{Hz}$". As a matter of fact,
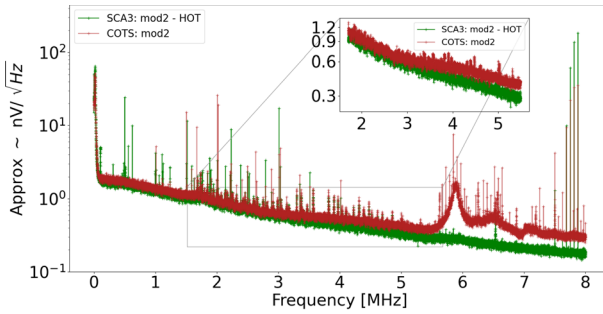
Fig. 6 Noise figure, configuration comparison: main relay (SCA#3-HOT, green) versus COTS (brown). The total level of noise with the tones is in the main box, while in the smaller one we plot the baselines noise (removing peaks) in a frequency range between ∼ 2 and ∼ 6 MHz
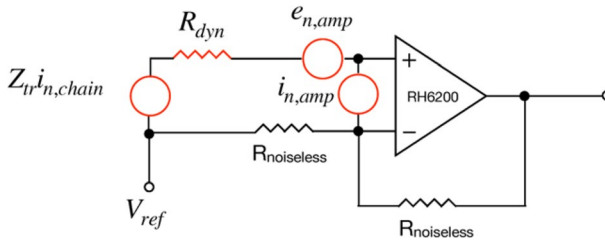

Fig. 7 Schematic model of the SCA in order to identify the main sources of noise

here we are interested in the ratio between the noise figures for different configurations of the boards.

As it is shown in the plots, boards with and without relay show a comparable level of noise, and the same happens when we compare both signal paths switched by the relay.

An upper limit on the added noise can be given by subtracting the two noise levels and is estimated to be below 0.1 nV/$\sqrt{Hz}$. When comparing INFN and COTS board, we see a slightly different frequency behaviour, the INFN prototype behaving slightly better in the region of interest (∼ 1 to 5 MHz).

4 SQUID-Independent Evaluation of SQUID Controller Assembly Noise

Since we are interested in the noise added by the electronics, independently of the actual SQUID used, we devised a method to characterize the noise level of the electronics board independent of the cold readout chain. Isolating the SCA noise in the real configuration allows us to compare it with future benchtop tests.

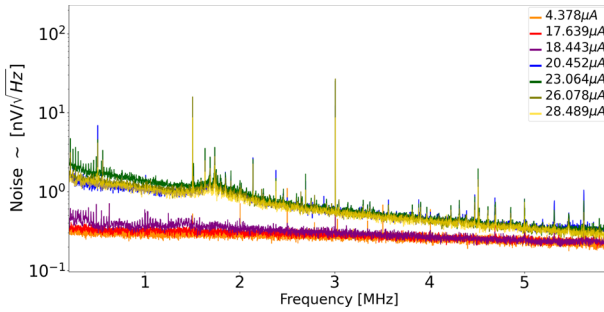The dominant sources of noise can be modelled as in Fig. 7.

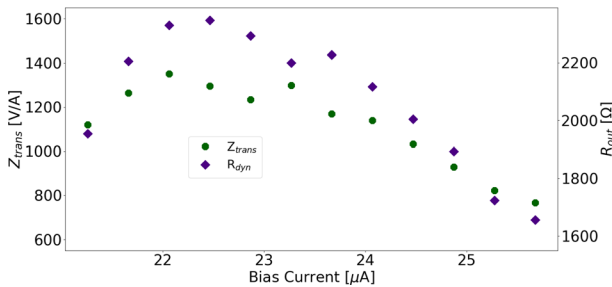**Fig. 8** Noise spectral densities for different currents bias

Fig. 9 Z_trans (blue) and R_dyn (green) for different values of the current bias

SCA noise is dominated by the input amplifier RH6200, chosen because of its low voltage and current noise and because it exists in a space-grade version. We distinguish three terms: the amplifier voltage noise (e_n), the amplifier current noise ($i_\text{n, ampl}$), and the cold readout chain current noise ($i_\text{n, chain}$). The latter two are affected by the SQUID characteristics and are amplified by the SQUID dynamical resistance and transimpedance, respectively, as visible from equation:

$$e_\text{total}^2 = e_\text{n}^2 + i_\text{n, ampl}^2\, R_\text{dyn}^2 + i_\text{n, chain}^2\, Z_\text{trans}^2 \tag{1}$$

To disentangle the different terms, we measured the noise in the full bandwidth as a function of the SQUID current bias (hence for different R_{dyn} and Z_{trans}). Figure 8 shows the noise for a sub-set (for ease of visualization) of the various current bias, and Fig. 9 shows R_dyn (green) and Z_trans (blue) for different values of the current bias. As an example, we report in Fig. 10 the noise squared in the [2, 2.5] MHz band, as a function of R_dyn^2 and Z_trans^2: we observe the linear behaviour expected from the simplified model. Fitting the slopes we can estimate the current and voltage noise. From the Z_trans^2 dependence, we obtain 8.4 10^{-2} pA^2/Hz and 0.50 nV^2/Hz, while for R_dyn^2 we get 3.6 10^{-2} pA^2/Hz and 0.44 nV^2/Hz. Although to extract the absolute noise value we have to take into account all the attenuation factors of the readout chain (some of which are still under evaluation), we can observe that the relative magnitude of the
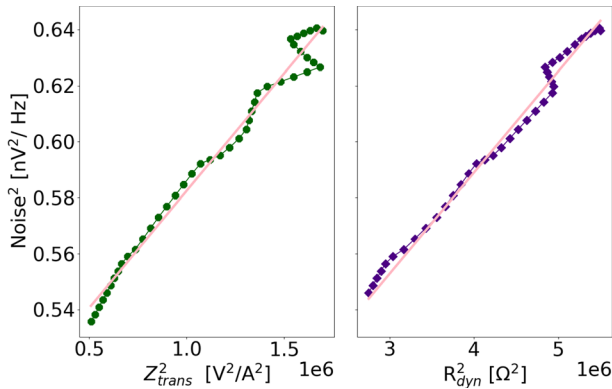
Fig. 10 Noise^2 in the band [2, 2.5] MHz as a function of Z^2_{trans} and R^2_{dyn}

contribution is compliant with the RH6200 specifications and with our cold readout chain.

5 Conclusion

We successfully tested our SCA breadboards demonstrating noise is not affected by the selected method to implement redundancy. In addition, our level of noise is comparable with COTS-based boards. We also presented a preliminary method to evaluate the boards noise without being affected by the cold chain in order to assess the intrinsic noise given by the SCA.

References

1. M. Hazumi et al., LiteBIRD satellite: JAXA's new strategic L-class mission for all-sky surveys of cosmic microwave background polarization. Int. Soc. Opt. Photon. **11443**, 114432 (2020). https://doi.org/10.1117/12.2563050
2. M. Tristram et al., Planck constraints on the tensor-to-scalar ratio. Astron. Astrophys. **647**, 128 (2021). https://doi.org/10.1051/0004-6361/202039585
3. M. Tristram et al., Improved limits on the tensor-to-scalar ratio using BICEP and Planck data. Phys. Rev. D (2022). https://doi.org/10.1103/physrevd.105.083524
4. C. LiteBIRD, Probing cosmic inflation with the LiteBIRD cosmic microwave background polarization survey. Prog. Theor. Exper. Phys. (2022). https://doi.org/10.1093/ptep/ptac150
5. G. Smecher, T. Haan, M. Dobbs, J. Montgomery, Digital Active Nulling for Frequency-Multiplexed Bolometer Readout: Performance and Latency (2022)
6. J. Montgomery et al., Performance and characterization of the SPT-3G digital frequency-domain multiplexed readout system using an improved noise and crosstalk model. J. Astronom. Telesc. Instru. Syst. (2022). https://doi.org/10.1117/1.jatis.8.1.014001
7. Q. Wang, M. Audley, P. Khosropanah, J. van der Kuur, G. de Lange, A. Aminaei, D. Boersmal, F. van der Tak, J.-R. Gao, Noise measurements of a low-noise amplifier in the fdm readout system for safari. J. Low Temp. Phys. **199**(3–4), 817–823 (2020). https://doi.org/10.1007/s10909-019-02328-x
8. T. Minotani et al., Effect of capacitive feedback on the characteristics of direct current superconducting quantum interference device coupled to a multiturn input coil. J. Appl. Phys. **82**(1), 457–463 (1997). https://doi.org/10.1063/1.365838

Authors and Affiliations

Giulia Conenna[1,2] · Andrea Tartari[3] · Giovanni Signorelli[3,4] · Andrea Passerini[1,2] · Andrea Limonta[1,2] · Mario Zannoni[1,2] · Paolo Dal Bo[3,4] · Eugenia Di Giorgi[3,4] · Jean-François Cliche[5] · Stefano Della Torre[2] · Matt Dobbs[5] · Luca Galli[3] · Massimo Gervasi[1,2] · Maurizio Massa[3] · Andrea Moggi[3] · Joshua Montgomery[5] · Donato Nicolò[3] · Michele Pinchera[3] · Graeme Smecher[6] · Franco Spinella[3]

✉ Giulia Conenna
  giulia.conenna@unimib.it

  Andrea Tartari
  andrea.tartari@pi.infn.it

  Giovanni Signorelli
  giovanni.signorelli@pi.infn.it

1   Physics Department, University of Milano Bicocca, Milano, Italy

2   INFN Milano Bicocca, Milano, Italy

3   INFN Pisa, Pisa, Italy

4   Physics Department, University of Pisa, Pisa, Italy

5   Department of Physics and McGill Space Institute, McGill University, Montreal, Canada

6   Three-Speed Logic Inc., Victoria, Canada